AAEC/E484

AAEC/E484

AUSTRALIAN ATOMIC ENERGY COMMISSION

RESEARCH ESTABLISHMENT

LUCAS HEIGHTS

DEVELOPMENT OF A SMALL, NANOSECOND TIMING

FAST NEUTRON SPECTROMETER

by

S. WHITTLESTONE

May 1980

ISBN 0 642 59686 7

AUSTRALIAN ATOMIC ENERGY COMMISSION
RESEARCH ESTABLISHMENT
LUCAS HEIGHTS

DEVELOPMENT OF A SMALL, NANOSECOND TIMING FAST NEUTRON SPECTROMETER

by

S. WHITTLESTONE

ABSTRACT

A neutron spectrometer has been developed for use inside a fast neutron assembly. The spectrometer is small and insensitive to gamma radiation.

An optical system was developed which could collect about 80 per cent of the light from an NE213 liquid scintillator and transmit it along a 450 mm quartz light guide to a high performance photomultiplier.

To enable the detector to be used as a nanosecond timing spectrometer, several calibration measurements were made of the detector efficiency and response to monoenergetic neutrons.

National Library of Australia card number and ISBN 0 642 59686 7

The following descriptors have been selected from the INIS Thesaurus to describe the subject content of this report for information retrieval purposes. For further details please refer to IAEA-INIS-12 (INIS: Manual for Indexing) and IAEA-INIS-13 (INIS: Thesaurus) published in Vienna by the International Atomic Energy Agency.

NEUTRON SPECTROMETERS; FAST NEUTRONS; NEUTRON DETECTION; NEUTRON SPECTRA; PULSED NEUTRON TECHNIQUES; FAST REACTORS

CONTENTS

(Continued)

1. INTRODUCTION

For an experiment to measure time-dependent neutron energy spectra in a pulsed fast neutron assembly of materials used in fast reactors it was decided that the best position for the detector was inside the assembly [Whittlestone 1979a]. This placed severe restrictions on the detector's physical dimensions and constituent materials to avoid perturbation of the neutron flux while obtaining satisfactory detector energy resolution and count rate.

The NE213 liquid scintillator (Nuclear Enterprises Ltd., Edinburgh, Scotland) was selected as the best type of detector. This report describes the determination of the limiting dimensions and the development of the detector, from glass and Perspex models, in which problems of detector filling and optical design were worked out, to the final version with optical components made from quartz. A suitable linear pulse height scale was selected and rather extensive calibrations required for a neutron spectrometer based on a liquid scintillator followed. Pulse shape discrimination (PSD) against gamma rays was used during the measurement of efficiency and monoenergetic neutron responses which resulted in a calibration of the combined detector plus pulse shape analyser system.

The use of PSD somewhat restricted the generality of the calibrations, and was not only unnecessary in some time-of-flight calibration measurements, but was actually a hindrance because it eliminated the gamma flash from the time-of-flight spectrum. However, these disadvantages were minor compared with the saving in effort, and increased confidence in results, gained by not having to correct the experimental data for effects due to the pulse shape analyser.

2. DESIGN CRITERIA

The requirements of the detector for the spectrometer were nanosecond timing resolution, minimal gamma-ray interference, and a sufficiently high efficiency to yield a 1 to 10 kHz count rate inside the metal assembly using the neutron source available. These requirements led to the choice of a NE213 liquid scintillator, which had the additional advantage of being formed readily into different shapes and sizes by using appropriate chambers.

The size of the scintillator required to give a count rate of a few kHz was calculated to be about 1 cm^3 using data from the experiment of Moo et al. [1973] with fission detectors in a thorium stack. This quantity of hydrogenous material causes an insignificant perturbation of the neutron energy spectrum in the uranium stack.

Having selected the scintillator, the next step was to choose a method of coupling the scintillator to the photomultiplier. Direct coupling was desirable because it would give optimum optical response. However, a light guide proved to be necessary for two reasons. Firstly, the gamma-ray flux in the stack was sufficient to generate large numbers of photoelectrons from the photocathode directly, creating an unacceptable background count rate. Secondly, the probe hole (26.4 mm^2) was too small for any commercially available photomultipliers with the performance demanded by the experiment. A larger probe hole would have caused more severe perturbation of the neutron flux, thereby precluding the possibility of calculating the flux by diffusion codes rather than by the more time-consuming Monte Carlo technique.

The only suitable material for the light guide is quartz, which is available with the extremely good light transmission essential for optimum energy resolution of the detector. Being composed of silicon and oxygen, quartz has fairly low neutron absorption and scattering cross sections and will not appreciably perturb the neutron flux.

The length of the quartz light guide (450 mm) was determined by the stipulation that a lead shield close to the photomultiplier should be at a distance from the stack comparable with the distance of other similarly massive items such as components of the stack support table and vacuum equipment.

3. DEVELOPMENT OF THE DETECTOR

The first experimental prototype detector was a small cylindrical glass chamber, with a volume of 0.45 cm^3, which was placed on the end of a Perspex light guide (the quartz was not yet available). The count rates were comparable to those estimated in Section 2. In a thorium stack, neutrons from the Be(d,n) source contributed about 10 kHz of a total count rate of 55 kHz. The remaining 45 kHz was examined by checking the count rate with different

arrangements of lead shields, with and without the scintillation chamber. Five kHz came from gamma-rays causing scintillations within the chamber and 40 kHz from gamma-rays passing down the Perspex rod to the photocathode. Calculations using mass absorption coefficients from Cember [1969] showed that replacement of the Perspex by quartz would reduce the gamma flux by a factor of 4. Since the optical properties of quartz are better than those of Perspex, the photomultiplier gain could be lowered to give the same response as the scintillator light output, so that the count from transmitted gamma-rays would be reduced by more than a factor of 4.

These tests of the first prototype showed that it was possible to obtain a reasonable count rate with a reasonable background using a detector of about 1 cm^3 volume. The steps taken from the first prototype to the final system to attain the best possible performance are now described.

3.1 Criteria for Assessing Detector System Performance

Two parameters define the quality of a detector system - the signal-to-noise ratio and the resolution. The first is directly proportional to the light output, L, of the scintillator optical system; it may be measured using a relationship due to Prescott [1963] linking the number, N, of photoelectrons from the photocathode to the mean, μ, and variance, σ^2, of the pulse height distribution obtained using a pulsed light source with constant amplitude,

$$N = 2\mu^2/\sigma^2 \quad . \tag{1}$$

If the quantum efficiency, η, is known, $L = N/\eta$. In the short term (a few months), η is constant for a given detector system, so N will be quoted as the scintillation system output. If the amplifier system gain is constant, N is proportional to μ. Thus:

$$N = k\mu \quad , \tag{2}$$

where k is a constant.

Measurement of N was effected by equipping the photomultiplier base assembly with a GaAs light emitting diode and a Perspex light guide (Figure 1). The value of k in Equation (2) was determined by measuring μ_a and σ_a of the response to fixed amplitude light pulses. Given k, the response μ_E to a

Compton electron of energy E from a gamma-ray source establishes the output N_E at energy E. The output, N_1, of the scintillation system to a 1 MeV electron is $N_E \times 1/E$.

The detector resolution, which limits its ability to differentiate between scintillation events of different amplitudes, is dominated by the variance, σ_p, of the pulse height distribution from light pulses of constant magnitude (Equation 1), together with the variance, σ_s, associated with non-uniformity of light collection efficiency over the volume of the scintillation chamber. The total resolution is:

$$\sigma_t^2 = \sigma_p^2 + \sigma_s^2 \quad . \tag{3}$$

The values of σ_s given in Table 1 were calculated from σ_p (Equation 1) and the total resolution, σ_t, of the response to the 0.511 MeV gamma-ray from ^{22}Na. The value of σ_t was obtained assuming the response to be a Gaussian broadened step or error function, which has as mean, μ, the half height and as variance, σ_t, which is 0.385 times the difference between the pulse heights at 10 and 90 per cent of the maximum count/channel; that is, $\sigma_t = N_{10}^{90} \times 0.385$. Although the values of σ_t and σ_s will all have a small systematic error because the response is not exactly an error function, the value of σ_s as a parameterisation of variation of light collection efficiency is in no way impaired.

A further aspect of resolution is edge effects. The 0.511 MeV gamma-ray rather than the 1.275 MeV gamma-ray was chosen for measuring σ_t because the ranges in the NE213 detector of the Compton electrons associated with these gamma-rays are up to 0.6 and 2.5 mm, respectively [Cember 1969]. The proportion of electrons hitting the walls of the chamber is small for the lower energy gamma-ray, but rather high for the other, in the small 10 mm diameter chambers. In the present experiment, edge effects are unimportant in the detection of neutrons because the range of a knock-on proton of 6 MeV is only 0.5 mm [Aron et al. 1949].

3.2 Performance of Different Detectors

Two relatively large detectors are described; their performance gives a standard against which later small detector performances can be compared.

Constructional details of the photomultiplier base assembly are shown in Figure 1 and the scintillation chambers and light guides in Figure 2. The pulse height spectra (Figure 3) were obtained from a ^{22}Na source (0.511 and 1.272 MeV gamma-rays) and a localised internal ^{113m}In Auger electron source; the latter is discussed in Appendix A. Before the chamber epoxy resin seals were applied, responses were obtained with the source rotated to various positions. The response between 5 and 15 mm from the photocathode varied by 29 per cent, whereas the response was constant when the source was between 15 and 30 mm. This suggested that a light guide 20 mm long might give more uniform light collection efficiency and so improve the system resolution. The light guide improved the uniformity of the ^{113m}In response, making the response closest to the photocathode 10 per cent larger than the response further away. However, the resolution for the uniformly distributed gamma source deteriorated slightly.

In a more successful attempt to design a chamber, a calculation was made of light reaching the photocathode just after one total internal reflection. If the walls of the chamber were conical rather than cylindrical, a substantial increase could be achieved. The performance of a cone with an angle of 15° to the axis showed a substantial increase (30 per cent) in light collection but, disappointingly, the system resolution deteriorated (Table 1).

It was clear, from the differences between performance and expectation with the large chambers, that either a much more rigorous program of basic experiments and calculations was required to optimise design for the scintillator probe, or a purely empirical approach should be employed. Only the latter was feasible at the time. A series of modifications was made to the light guide of the small glass chamber, culminating in the system shown in Figure 2(f), which performed inadequately (Table 1). Not only was the transmission poor (29 per cent), but the system resolution, 0.18 (σ/μ), which reflects variation in light collection efficiency, was unacceptable. The chamber without the guide performed quite well, but even the 25 mm section of light guide used to interface the detector to the guide, worsened the resolution considerably. A new design was required.

Some guidance was sought from a quite rigorous computer calculation of several detector optical systems by Falk and Spartman [1970]. Their results were not in qualitative agreement with the present results (Table 1). For example, with sampling along the walls of the chamber, Falk and Spartman

predicted that a conical chamber would have better resolution than the cylindrical chamber. In Table 1 it can be seen that the resolution of the large conical chamber with a uniform source was worse. Despite this discouragement, and the observation that crazing to a depth of approximately 1 mm occurred overnight in Perspex soaked in NE213 liquid, the conical Perspex chamber in Figure 2(g) was made and tested.

The performance was remarkably good. Not only was the light output as good as that of the large glass chamber, but also the system resolution was more than a factor of two better. Figure 4 shows the responses to a ^{22}Na source of the Perspex cone, the small glass chamber with the interface only and the latter chamber with the full 470 mm guide. Even with the full Perspex guide, the resolution of the Perspex cone chamber was worsened by only a factor of 1.1, as opposed to 2.0 when the small glass chamber was used. When the full 450 mm quartz guide became available and was coupled to the conical Perspex chamber, it proved possible to transmit 81 per cent of the light without loss of resolution. The response to a ^{113m}In source with and without the quartz light guide is shown in Figure 5.

Two chambers were made from quartz to the dimensions of the Perspex cone. A pulse height spectrum from a ^{22}Na source is given in Figure 6. The performance was similar to that of the large glass chamber, the overall resolution of the 0.511 MeV gamma-ray being the same, the system resolution of the quartz cone better and its response, N, smaller. Details of the construction of the scintillator probe are given in Figure 7. The only difference between the two quartz chambers was the degree of polish on the inside surface, enabling the second chamber to give 10 per cent more light output.

In view of the difficulty of constructing the hollow quartz cone, and the remarkable life of the Perspex cone chamber which was still working after three years, it would be better to construct the small hollow part of the chamber from Perspex. The extra hydrogenous material would not matter (approx. 1 cm^3) and the benefit of easier construction would outweigh the trouble of replacing the Perspex chamber every year or so, should crazing lead to serious damage to the chamber.

4. PULSE HEIGHT SCALE AND THRESHOLD

There are at least three reasonable choices of pulse height scale against which measurements could be calibrated. Most directly relevant to the measurements would be the response of the detector to protons, because the upper edge of the proton energy distribution from a monoenergetic neutron is equal to the energy of the neutrons. However, the proton response of a liquid scintillator is strongly non-linear in terms of pulse height and is inconvenient to work with.

Many authors prefer to use a scale which is linear in pulse height (for example, Verbinsky et al. 1968). They define a 'light unit' in terms of the response of the scintillator to a gamma-ray. The objection to this scale is a matter of taste; the 'light unit' is not so much a measurement of light output as a name given to a linear scale on which the response to a 1.25 MeV electron is 1 unit.

In general, if the pulse height scale is to be linear, some secondary unit, such as light output, must be used. However if, as in the present measurements, the lower energy threshold is set to ignore pulses less than the response to a 100 keV electron, the electron response itself is linear and therefore suitable as a scale.

Although there is general agreement that the electron response is linear above about 100 keV, there is some suggestion that the extrapolated response has a non-zero intercept at zero energy, which rather spoils the electron response as an ideal scale. Measurements by Flynn et al. [1964] using Auger electrons in the range 0.026 to 0.01 MeV, and by Horrocks [1974] using Auger electrons and Compton electrons in the range 0.0065 to 0.636 MeV, both indicated that the response was linear above 0.1 MeV, but that the linear region had an extrapolated zero intercept at about 20 keV. Measurements to check this, using Compton electrons in the range 0.341 to 1.61 MeV, yielded a straight line with an intercept at -4 ± 5 keV. Within the accuracy of these measurements, the electron response over 0.341 MeV is directly proportional to pulse height; accordingly, the unit of pulse height used throughout this paper is the response of the detector to a 1 MeV electron-designated $\underline{H}_e$.*

* The '$\underline{H}_e$' is identical to 'MeVe' used elsewhere [cf. Whittlestone 1980], and accords with AAEC practice in choice of notation.

During the experiments, the pulse height scale was calibrated with a ^{137}Cs source. This isotope produces a single gamma-ray of 0.6616 MeV which is the maximum energy usable in the small detector because of edge effects.

The upper end of the range of pulse heights in $\underline{H}_e$ was determined by the response to the highest energy neutrons to be measured - about 4 $\underline{H}_e$ for 6.5 MeV neutrons. Edge effects were unimportant for neutrons of this energy because of the short range of protons in the scintillator. The dynamic range of the analogue to digital converter (ADC) and timing walk of the constant fraction of pulse height triggers (CFTs) limited the lower level discriminator to a minimum of 0.1 $\underline{H}_e$. This permitted measurements of neutrons down to 0.5 MeV.

5. DETECTOR EFFICIENCY

As mentioned in Section 1, the detector efficiency was measured with the pulse shape analyser connected. Preliminary measurements indicated that the best compromise between high gamma rejection and low neutron loss was when the pulse shape analyser was set to reject 98 per cent of the counts from the ^{137}Cs calibration source.

The most expedient way to measure the probe efficiency was to compare energy spectra taken by the probe and the large NE213 detector simultaneously, using time-of-flight analysis. Since the efficiency of the latter is known [Whittlestone 1977], the efficiency of the probe was readily determined from the ratio of the two spectra.

Some difficulty was experienced with this measurement because of the considerable difference in count rates (100:1) when the detectors were side by side. To obtain a reasonable count rate from the probe while limited to a total rate of 5 kHz by the pulse height analyser, it was necessary to place the large detector at 2 m and the probe at 1 m from the target. This gave rise to a difference in energy resolution which, for two reasons, was not considered to be important. Firstly, the efficiency does not change rapidly with energy and secondly, the neutron energy spectrum from a lithium target bombarded by 2.3 MeV deuterons (Figure 8) was free from fine structure over the region of interest.

Another problem associated with the count rate difference was the correction for dead time in the pulse height analyser. This was overcome by setting up time gates and delays so that the time spectra from both detectors were collected, in the same time spectrum, from the same time-to-amplitude converter. Dead time losses were equal throughout the composite spectrum. Corrections arising from multiple events per neutron burst were calculated to be less than 1 per cent and were ignored.

The efficiency derived from the comparison with the large NE213 detector (Figure 9) was checked by two means. Firstly, a Monte Carlo calculation, using the proton responses of Smith et al. [1968] was made by Clayton [1977]. This was within 10 per cent of the experimental points up to 7 MeV. Secondly, the energy spectrum from a beryllium target was measured using the scintillator probe and compared with the previous measurement [Whittlestone 1976]. The two spectra, shown in Figure 10, agree very well above 0.7 MeV, provided that allowance is made for the slightly improved resolution of the measurement with the small detector.

These two confirmations of the efficiency measurement are consistent with the accuracy of 7 per cent between 0.7 and 7 MeV calculated from measurement errors (5 per cent) and the accuracy with which the large detector efficiency was known (5 per cent).

6. MONOENERGETIC NEUTRON RESPONSES

The indispensable element of neutron spectroscopy with an organic scintillator is the monoenergetic neutron response matrix. Any errors in this matrix are reflected directly into the unfolded energy spectrum. During the period since about 1960, when the value of organic scintillators as spectrometers was first appreciated and exploited, many different experimental and theoretical techniques have been tried in an attempt to establish the response of scintillators to monoenergetic neutrons. This section is devoted to a brief exposition and evaluation of different techniques, followed by a detailed account of the derivation of the responses used in the present measurements. The initially promising method of calculating the responses with a Monte Carlo code and making a few check measurements was abandoned in favour of an almost entirely experimental determination of the responses.

Monte Carlo methods have been adopted almost universally for calculating responses. Batchelor et al. [1961], who virtually pioneered neutron spectroscopy with organic scintillators, tracked neutrons until they escaped or were absorbed. They added into the scintillator light output the contributions from recoil protons, recoil carbon nuclei, and alphas from the $^{12}C(n,\alpha)^{9}Be$ reaction. Textor and Verbinsky [1968], and later Kellerman and Langkau [1971], further refined the detector model to include all significant neutron-carbon interactions, as well as effects due to recoil protons leaving the scintillator. In these calculations, the variation in light collection efficiency, or resolution, of the scintillation chamber has been modelled by a Gaussian broadening function with empirically determined parameters. De Leo et al. [1974] have extended their Monte Carlo code to allow for light attenuation of the scintillator and for reflection losses.

These calculations agreed rather well with the one or two accompanying examples of experimentally determined responses. A Monte Carlo code was written [E. Clayton, AAEC private communication 1972] to simulate a scintillation detector of dimensions 36 x 50 mm diameter for neutron energies in the range 0.02 to 10 MeV. The detector size and neutron energy range allowed edge effects and carbon (n,α) reactions to be neglected. It was decided to treat the resolution of the system more rigorously than had been done before, using the resolution function of Prescott [1963] to allow for the photomultiplier statistics with the variance obtained from light pulser measurements (Section 3, Equation 1). A fixed variance term was used to account for the pulse height independent resolution at large pulse heights (neutron energies > 2 MeV in the present case).

The magnitude of this last term, which accounts for variation in light collection efficiency, was determined empirically because it was difficult to calculate. For example, results obtained with different size chambers suggested, contrary to the work of de Leo et al. [1974], that the dominant losses are due to reflectivity of the chamber walls and not to light attenuation within the chamber. In Table 1, it will be noted that the results for total light output, the best indicator of total attenuation, are practically the same for different sizes of the same geometry. For these chambers, therefore, the total light path length is unimportant. The task of calculating light collection efficiency was evidently a major problem in itself, with discrepancies between the above results and those of others to be resolved.

Calculations of monoenergetic neutron responses were made for the large glass chamber, since this was comparable with the size of chambers, whose responses had been calculated by other workers. First, light output data from proton reactions were taken from Smith et al. [1968]. When these failed to produce good agreement with experimentally determined monoenergetic neutron responses, the calculation was made using different proton responses reported by Batchelor et al. [1961] and Verbinsky et al. [1968]. Finally, some empirical modifications of the published proton responses were used. The results for two energies with responses by Smith et al. [1968] and one of the modified response sets are shown in Figures 11(a) and (b). There appeared to be no simple way to modify the published proton responses to obtain agreement between experiment and theory. It was evident that calculations could not be made successfully unless a set of proton responses was measured. But the most widely used techniques for measuring proton responses produce, directly or with minor modification, monoenergetic neutron responses. In the present case, since the main interest was neutron spectra rather than the detectors, it was decided to forgo response calculation in favour of direct measurement.

The most suitable techniques available were either to define a monoenergetic neutron flux using the deuterons associated with neutron emission from the $D(d,n)^3He$ reaction, or to separate out neutron energies by time-of-flight. In practice, the former technique yielded too low a count rate, but the latter gave inadequate energy resolution on neutrons with energies above 2 MeV.

The approach taken was to use time-of-flight energy separation to establish a basic set of neutron responses (set A). These responses were corrected using available information about resolution and proton responses from gamma-ray measurements and from some measurements with very poor statistical accuracy obtained using the associated particle technique (Appendix B). A function was found whose parameters could be varied to represent the response for each neutron energy. These parameters were then adjusted using the available information to obtain parameters from which a new set of responses could be generated. As a starting point in the adjustment procedure, it was assumed that the parameters should vary smoothly with neutron energy. Next, the proton responses at higher neutron energies were brought into consistency with the responses from the associated particle measurements.

Finally, the response matrix was folded with a test energy spectrum from a time-of-flight measurement, to generate a pulse height spectrum. The latter should agree with the pulse height spectrum obtained with the neutron source used for the test energy spectrum. Slight adjustments were made to the response matrix to obtain agreement with test data.

The basic function chosen to model the responses was selected from combinations of exponentials, broadened step functions and sloping lines, using a program SUPERFIT by Clancy [1977], which is an interactive code designed for just this type of problem. The best function proved to be:

$$Y(x_i) = A \cdot e^{T(p-x_i)} + B \cdot e^{U(p-x_i)} + C \cdot \mathrm{erf}\left[\frac{Q-x_i}{S}\right] , \qquad (4)$$

where $Y(x_i)$ = count in channel i,

x_i = pulse height of channel i, and

A, B, C, P, Q, S, T, U are parameters to give the best fit to the experimental data.

The function is illustrated in Figure 12(a). Of the eight parameters, the only two with obvious significance are Q, the proton response, and S, the latter being twice the variance of the photomultiplier plus scintillator response.

Having selected the function, a specialised subroutine PFIT based on VA06A by Powell [1970] was written for the data handling code AND [Whittlestone 1979(b)]. It was found that, by using PFIT, only one exponential term was necessary for neutron energies up to 1.6 MeV. Thus for the lower energies, five parameters were fitted, P being set at the threshold 0.1 $\underline{H}_e$, while B and U were set to zero. For neutron energies of 1.9 MeV and greater, both exponential terms were needed, but only one more parameter proved to be necessary, it being best to fix the Y value at x = P; i.e.

A+B+C = experimental Y(P).

Each of the parameters from PFIT was treated as a function of neutron energy and fitted to the polynomial in energy of whichever order (up to 4) gave the best fit. In the case of the upper edge variance parameter, S, the fitted values were taken for neutron energies up to 1.374 MeV, where S/Q reached its minimum value of 0.19. Since edge effects were negligible, the only mechanism for an increase of S/Q with energy was time-of-flight energy

dispersion. Thus for higher energies, S was put equal to 0.190. The proton response, Q, was taken from the fitted values up to 3.62 MeV and from the associated particle measurement above that energy. Figure 13 shows the values of S and Q obtained from the measured profiles, as well as the best polynomial fit to these parameters, and the values taken to generate the monoenergetic response set B. Each response was scaled so that the integral above the threshold equalled the efficiency previously measured for each energy (Section 5).

The final phase of establishing the response set was to make slight adjustments to the proton response (Q) and resolution (S) parameters, to obtain consistency in the test spectrum measurement. Adjustments of Q of the order of a few per cent were consistent with the data from the time-of-flight measurements. The value of S could be calculated by assuming chamber resolutions, σ/μ, in the range 0.04, which was measured using the gamma-ray responses (Table 1) to 0.08, as suggested by the associate particle measurement. The photomultiplier resolution was calculated using N_1 = 1010 (Table 1), because this value was considered accurate and gave good agreement with the time-of-flight measurement at low energies, where the photomultiplier resolution was dominant.

The test spectrum chosen was the $^{9}Be(d,n)^{10}B$ reaction at angle 0°, because the spectrum was both well known and complex enough to be a challenge to the spectrum measurement technique. Figure 14 shows the difference between the measured pulse height spectrum and a reconstructed pulse height spectrum obtained by folding the energy spectrum with the response set A. Also shown are the differences resulting from folding with set C, a slight modification of the generated set B (the chamber resolution, σ/μ, was decreased from 0.13 to 0.08) and with set D, which was obtained by optimising both Q and the chamber resolution.

A valuable index of compatibility of two spectra is the sum of the squares of the differences divided by the number of points - χ^2/N. Values of χ^2/N for each response set were obtained by scaling the folded pulse height spectrum to minimise χ^2/N above pulse heights of 0.60 $\underline{H}_e$; this corresponds to neutrons with energies above the big step in the $^{9}Be(d,n)^{10}B$ spectrum at 1.5 MeV. χ^2/N values were then calculated for the sections of the spectrum between 0.25 and 0.6 $\underline{H}_e$. In the region between threshold and 0.25 $\underline{H}_e$, no optimisation was carried out because the responses were no longer step-like

and thus insensitive to change in Q after scaling to preserve the efficiency. The sensitivity of χ^2/N to small changes in Q and rather larger changes in chamber resolution is apparent in Table 2. Table 3 gives a complete set of parameters used to generate response set D and the changes in Q and S from set C, the set generated from the response function parameterisation with only the chamber resolution being optimised.

7. CONCLUSIONS

The most important points to emerge are:

(a) The whole complex process of deriving the monoenergetic neutron responses is vindicated by the success in creating a profile set which can be folded with an energy spectrum to match a measured pulse height spectrum within a few per cent over most of the pulse height range (Figure 14).

(b) A relatively simple function (Equation 3) has proved adequate to represent the response of the scintillator probe for neutrons up to about 6 MeV.

(c) The technique of reconstructing a pulse height spectrum by folding an energy spectrum with a profile set provides not only a test of the profiles, but also a means of finely adjusting the profiles in regions where they are most subject to error.

(d) Relatively small changes in the proton responses, Q, lead to very large χ^2/N values from the experimental and refolded pulse height spectra (Table 2). A corollary of this, of some importance in discussion of iterative techniques for the unfolding of data to produce energy spectra, is that an unfolded spectrum may be quite close to the ideal solution to the unfolding problem and yet produce a very large value of χ^2/N. In other words if, as is usually the case, the reconstructed pulse height spectrum does not agree very well with the experimental data, the energy spectrum may still be acceptably accurate.

8. ACKNOWLEDGEMENTS

I am indebted to Mr W. Gemmell for his support throughout the work. Of the many members of the AAEC Physics Division who assisted, I wish to thank particularly Dr A.I.M. Ritchie, Dr D. Lang and Dr B.E. Clancy for valuable discussions, and Mr A. Van Heugten, Mr J. Fallon and Mr H. Broe for helping to keep the accelerator operational. The assistance of Mr D. Stevenson in constructing the detector system, Mr R.J. Cawley and Mr M.D. Scott with the on-line computer, Mr G.D. Trimble with FORTRAN programming, and Mr E. Clayton with detector calculations was invaluable.

I also wish to thank Mr D. Stathers for the glass scintillation chambers and Mr H. Wyllie for the gamma-ray and detector calibration sources.

9. REFERENCES

Aron, W.A., Hoffman, B.G. and Williams, F.C. [1949] - AECU-663.

Batchelor, R., Gilboy, W.B., Parker, J.B. and Towle, J.H. [1961] - Nucl. Instrum. Methods, 13:70.

Cember, H. [1969] - Introduction to Health Physics, Pergamon Press; p.110.

Clancy, B.E. [1977] - AAEC/E408.

Falk, F. and Spartman, P. [1970] - Nucl. Instrum. Methods, 85:253.

Flynn, K.F., Glendenin, L.E., Steinberg, E.P. and Wright, P.M. [1964] - Nucl. Instrum. Methods, 27:13.

Horrocks, D.L. [1964] - Nucl. Instrum. Methods, 30:157.

Jones, D.T.L. and Bartle, C.M. [1974] - Nucl. Instrum. Methods, 118:525.

Kellerman, H.J. and Langkau, R. [1971] - Nucl. Instrum. Methods, 94:137.

de Leo, R., d'Erasmo, G., Pantaleo, A. and Russo, G. [1974] - Nucl. Instrum. Methods, 119:559.

Moo, S.P., Rainbow, M.T. and Ritchie, A.I.M. [1973] - J. Nucl. Energy, 27:753.

Powell, M.J.D. [1970] - AERE-R6469.

Prescott, J.R. [1963] - Nucl. Instrum. Methods, 22:256.

Smith, D.L., Polk, R.G. and Miller, T.G. [1968] - Nucl. Instrum. Methods, 64:157.

Textor, R.E. and Verbinsky, V.V. [1968] - ORNL-4160.

Verbinsky, V.V., Burrus, W.R., Love, T.A., Zobel, W., Hill, N.W. and Textor, R. [1968] - Nucl. Instrum. Methods, 65:8.

Whittlestone, S. [1976] - AAEC/E399.

Whittlestone, S. [1977] - AAEC/E420.

Whittlestone, S. [1979(a)] - AAEC/E490.

Whittlestone, S. [1979(b)] - AAEC/E489.

Whittlestone, S. [1980] - Nucl. Instrum. Methods, 169:215-218.

TABLE 1

PROPERTIES OF THE SCINTILLATION CHAMBERS

Chamber	Volume (cm^3)	Light Guide (Figure 2)	Output N_1*	Resolution† σ/μ			Comments
				System σ_s/μ	0.511 MeV γ from ^{22}Na σ_t/μ	0.392 MeV electron σ_t/μ	
Large glass cylinder	65	-	1410	0.060	0.088	0.094	Perspex light guide reduced response by 25% and slightly worsened resolution.
		20 mm Perspex	1052	0.069	0.102	0.096	
Large truncated cone	38	-	1880	0.074	0.093	-	Light collection efficiency improved by 30%, but resolution worsened.
Small glass cylinder	0.45	-	1540	0.068	0.092	0.126	Performance essentially the same as the large glass cylinder.
		25 mm Perspex	1100	0.102	0.126	-	28% loss in response and considerable loss of resolution due to guide.
		470 mm Perspex	440	0.18	0.21	0.27	Very poor response and resolution.
Perspex cone	0.58	Integral 25 mm Perspex	1430	0.025	0.069	0.122	Improved optics increased response and resolution
		470 mm Perspex	570	-	-	0.136	Response too poor to locate knee in response. 40% transmission.
		200 mm quartz	1240	-	-	0.123	Resolution unimpaired by guide. 87% transmission.
		450 mm quartz	1080	-	-	0.115	Resolution improved. 81% transmission.
Quartz cone No. 1	0.58	450 mm quartz	893	0.041	0.091	0.121	Light output reduced by imperfect inner surface of cone.
Quartz cone No. 2	0.58	450 mm quartz	1010	0.042	0.087	-	Optical performance same as Perspex cone, but no hydrogen!

*N may be regarded as the number of photoelectrons emitted from the photocathode when an electron of 1 MeV is stopped in the scintillator (equation 3.1).

†The procedure for obtaining σ is discussed in the text, section 3.3. Accuracy ∿5%.

The electron source, ^{113m}In, was on a platinum wire inside the chamber. The resolution depended on the position and so this source is useful only for comparison of performance of a particular chamber under varied conditions, but not for comparing two chambers.

TABLE 2

VALUES OF χ^2/N FOR FOLDED PULSE HEIGHT SPECTRA
COMPARED WITH TEST SPECTRUM FROM $^{9}Be(d,n)^{10}B$ REACTION

Mono-energetic Neutron Response Set	Comment	Chamber Resolution	χ^2/N Optimised in range 0.6-3.5 H_e Pulse Height Range (H_e)		
			0.25-0.60	0.60-3.5	0.25-3.5
Time of flight					
A		0.19	1125	46	160
C		0.08	280	24	51
F		0.08	19	2.4	4.1
D	Q changed by a few % (see Table 3)	0.06	9.9	1.6	2.5
E		0.04	20	2.5	4.3

TABLE 3

PARAMETERS OF MONOENERGETIC NEUTRON RESPONSE SET D

Response No.	Neutron Energy	Proton Response Q ($\underline{He}$)	% Charge from set C	Other Parameters (see equation 3.3) P = 0.10 MeVe						
				A x 10^3	B x 10^3	C x 10^3	S ($\underline{He}$)	% Charge from set C	T ($\underline{He}^{-1}$)	U ($\underline{He}^{-1}$)
1	0.535	0.1060	+3.2	6.138	4.719	4.719	0.0239	-3.7	70.08	70.08
2	0.619	0.1303	3.2	5.021	3.824	3.824	0.0269	-3.7	61.32	61.32
3	0.721	0.1617	3.1	3.969	2.970	2.970	0.0304	-4.9	51.39	51.39
4	0.854	0.1853	-7.3	3.076	2.262	2.262	0.0316	-15	44.38	44.38
5	1.032	0.2310	-9.2	2.297	1.655	1.655	0.0367	-19	36.50	36.50
6	1.188	0.3088	-4.6	1.842	1.304	1.304	0.0440	-16	31.83	31.83
7	1.374	0.4008	0	1.461	1.016	1.016	0.0533	-13	28.62	28.62
8	1.622	0.5018	-2.1	1.116	0.7605	0.7605	0.06215	-16	26.28	26.28
9	1.922	0.6719	+2.0	0.8919	0.6104	0.5621	0.0780	-14	25.55	2.175
10	2.23	0.8760	-1.0	0.6688	0.4533	0.4002	0.0958	-17	26.28	2.132
11	2.87	1.232	+4.7	0.4880	0.3304	0.2707	0.1273	-15	28.91	2.073
12	3.62	1.673	+4.2	0.3550	0.2444	0.1756	0.1651	-17	32.85	2.015
13	4.76	2.185	-3.6	0.2588	0.1872	0.1046	0.2066	-25	37.23	1.883
14	6.44	3.240	-2.3	0.2048	0.1614	0.0586	0.2974	-24	40.88	1.737

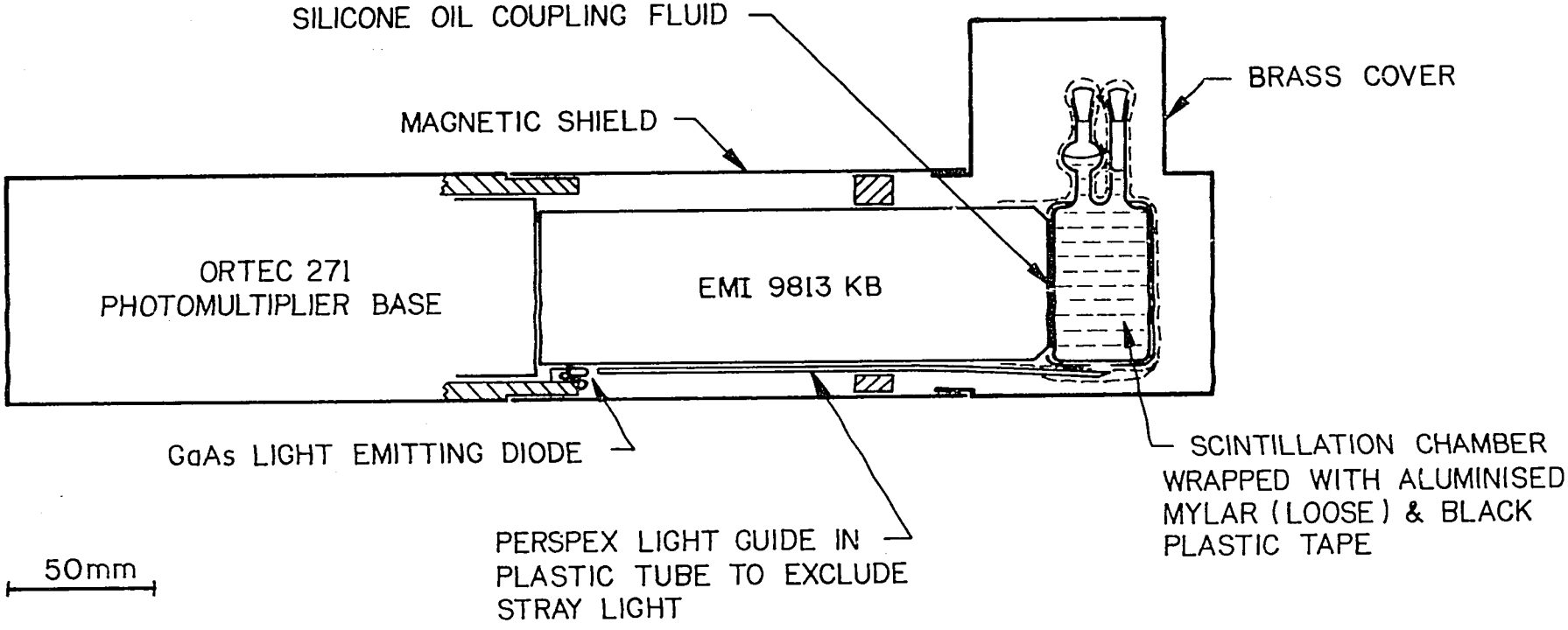

FIGURE 1. PHOTOMULTIPLIER BASE ASSEMBLY

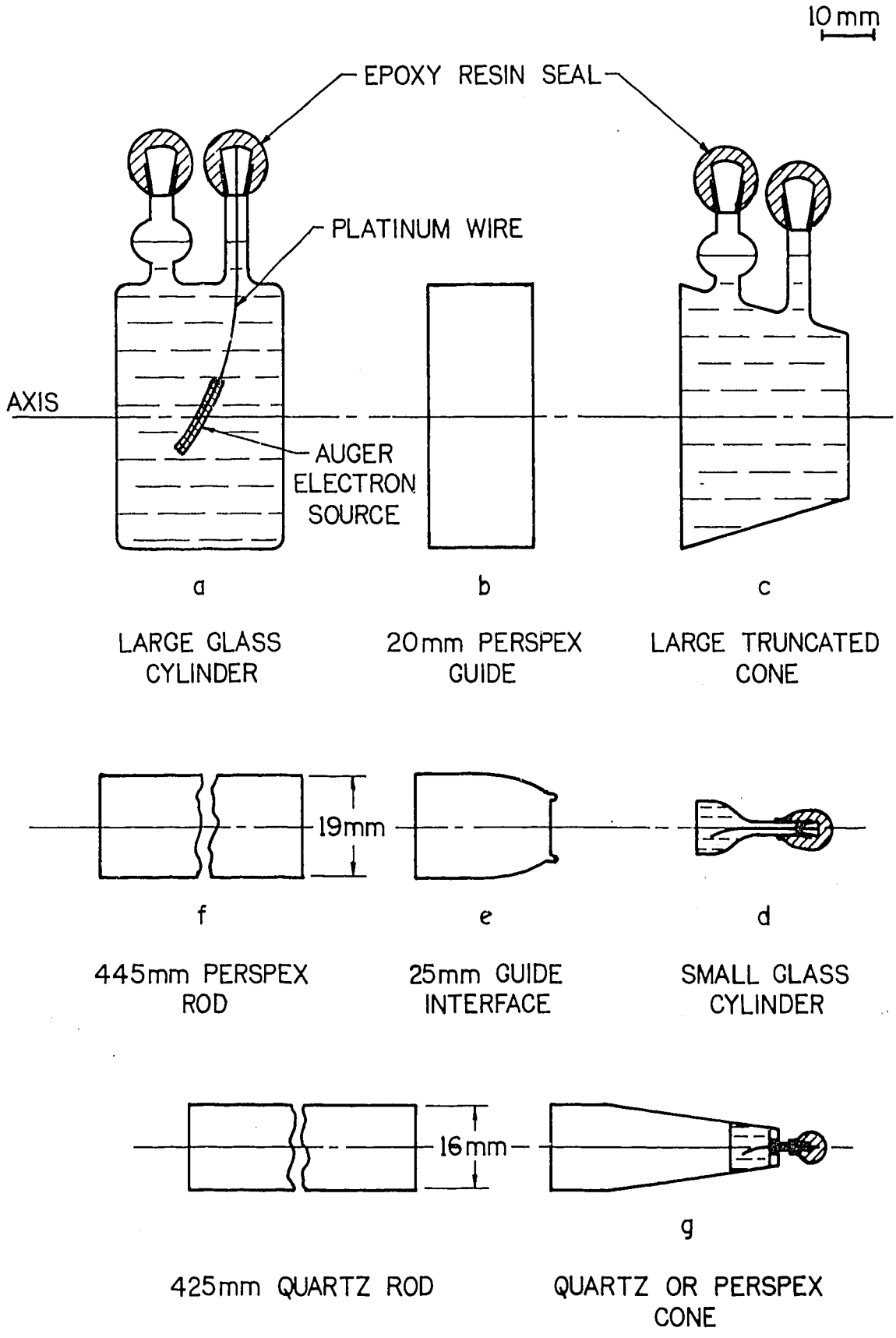

FIGURE 2. THE SCINTILLATION CHAMBERS AND LIGHT GUIDES

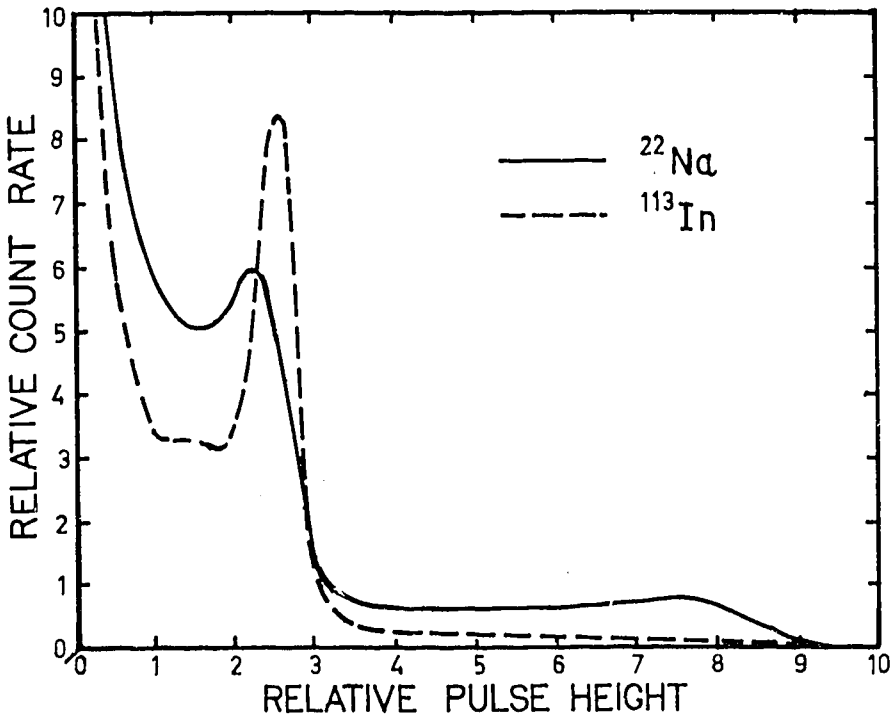

FIGURE 3. PULSE HEIGHT DISTRIBUTIONS FROM LARGE GLASS CYLINDRICAL DETECTOR

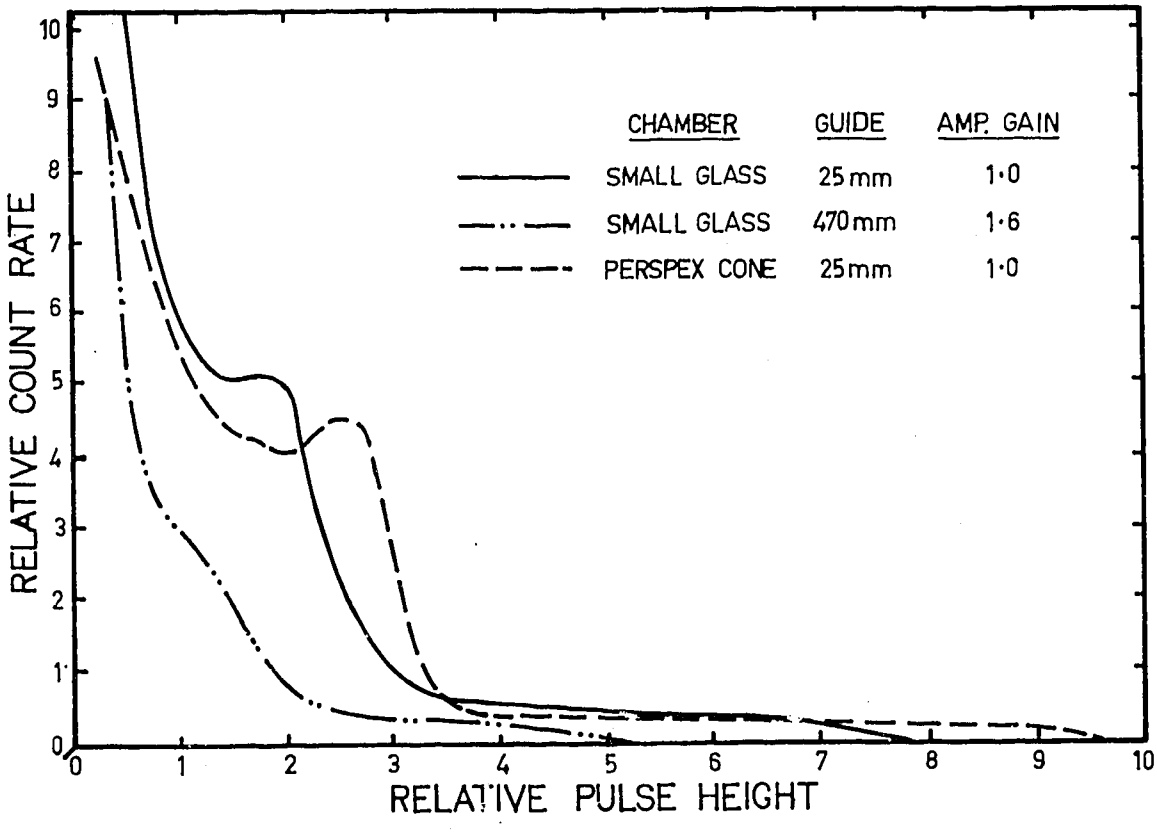

FIGURE 4. ^{22}Na RESPONSES OF SMALL GLASS AND PERSPEX CONE CHAMBERS

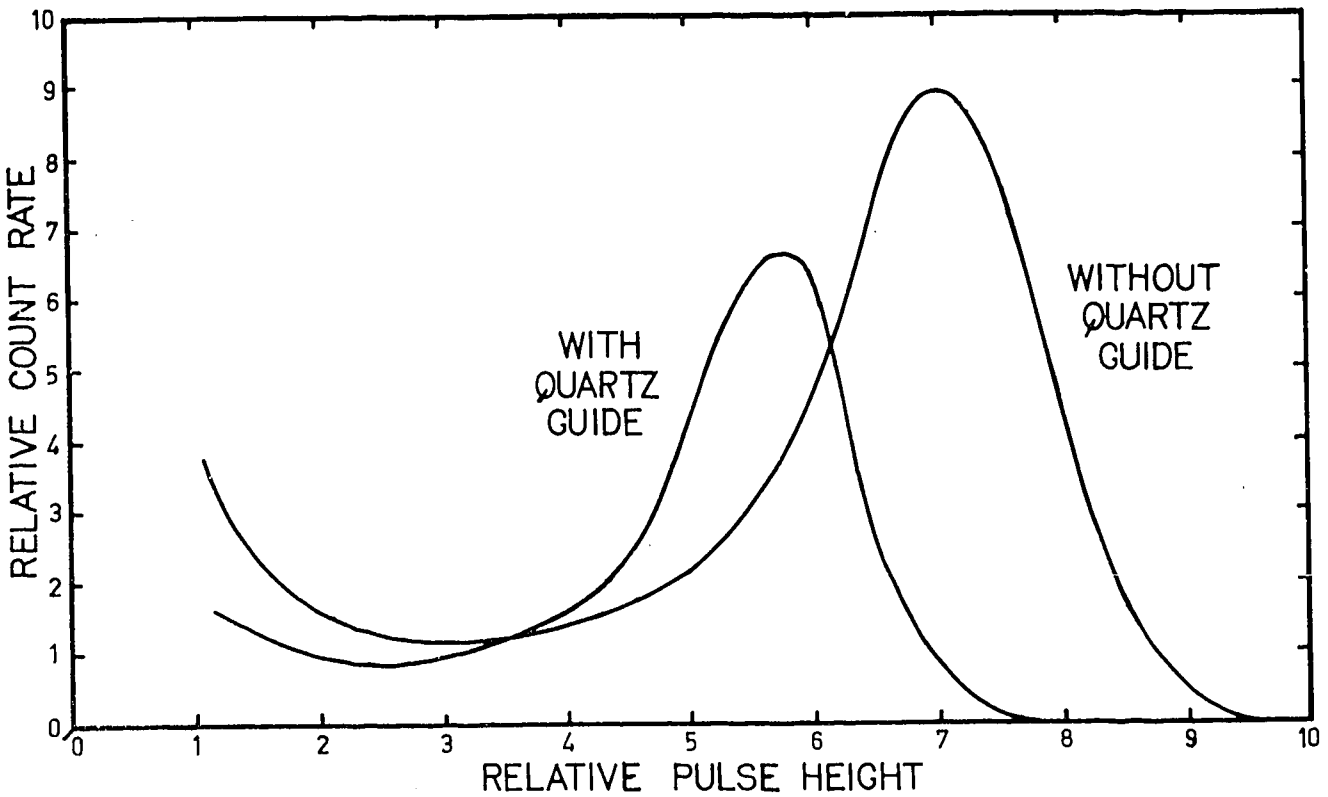

FIGURE 5. QUARTZ LIGHT GUIDE TEST RESPONSE OF PERSPEX CONE TO ^{113}In SOURCE

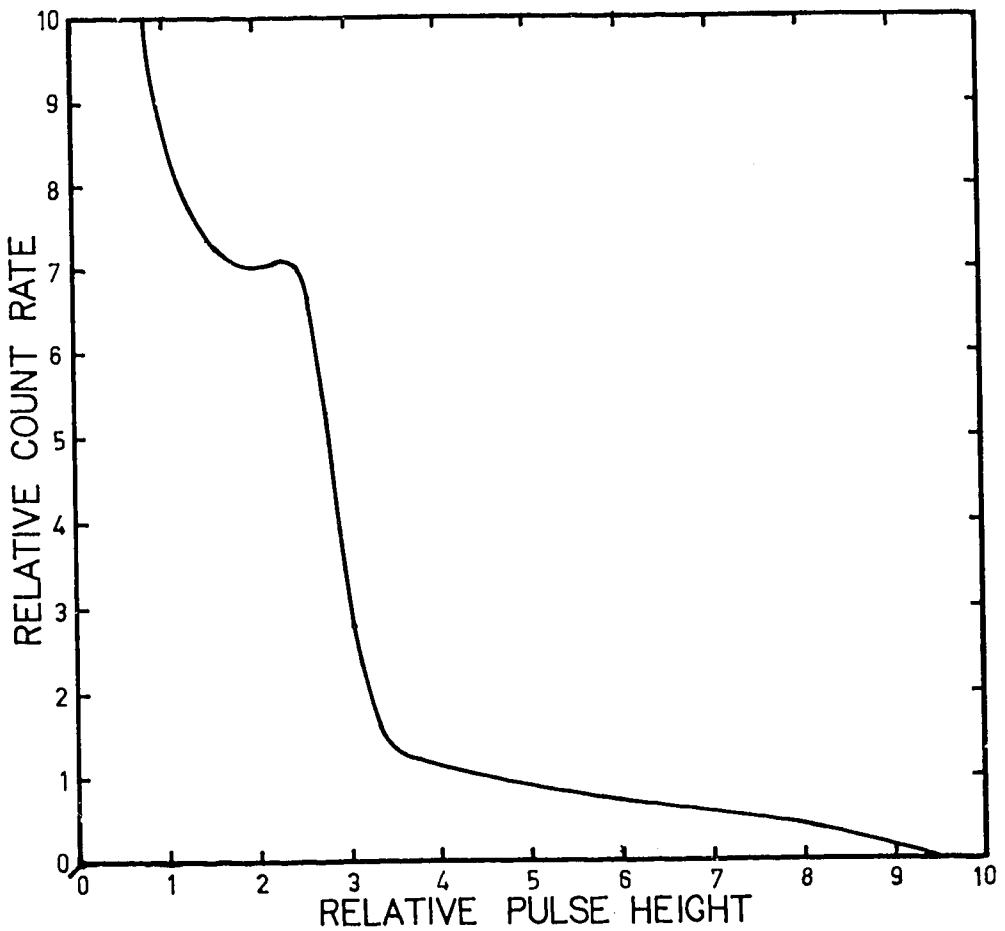

FIGURE 6. RESPONSE OF QUARTZ PROBE DETECTOR TO ^{22}Na SOURCE

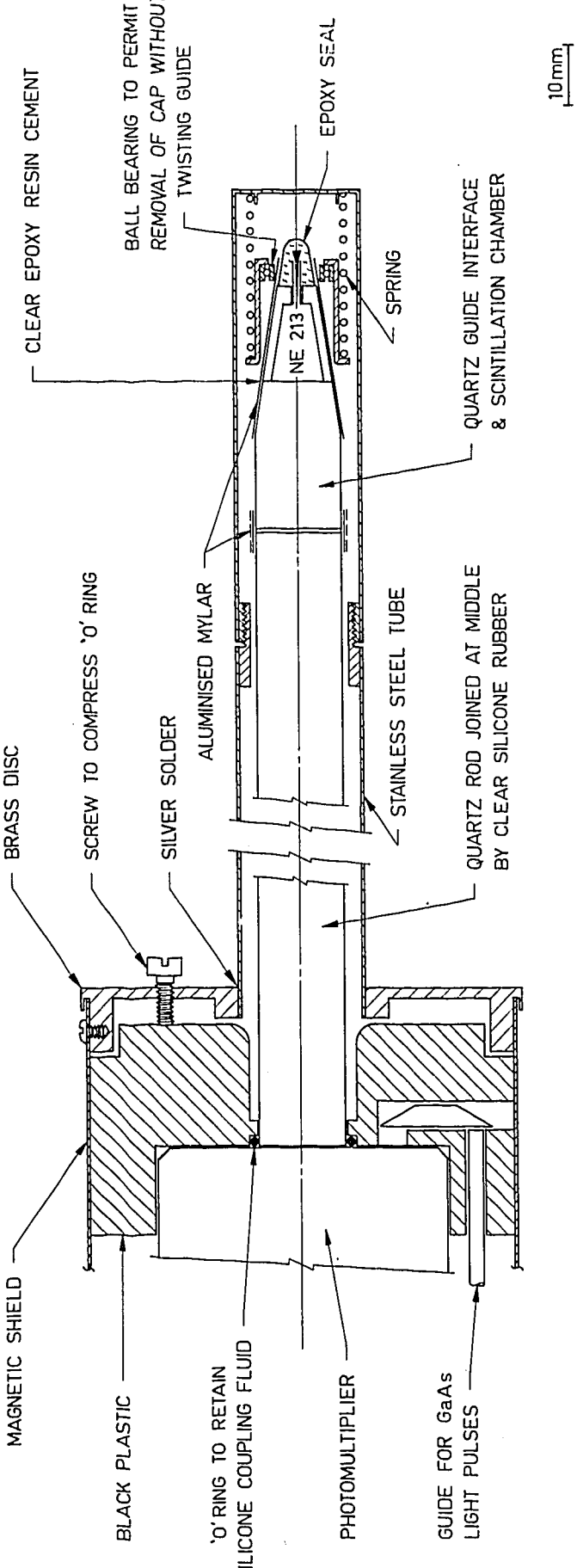

FIGURE 7. THE SCINTILLATOR PROBE

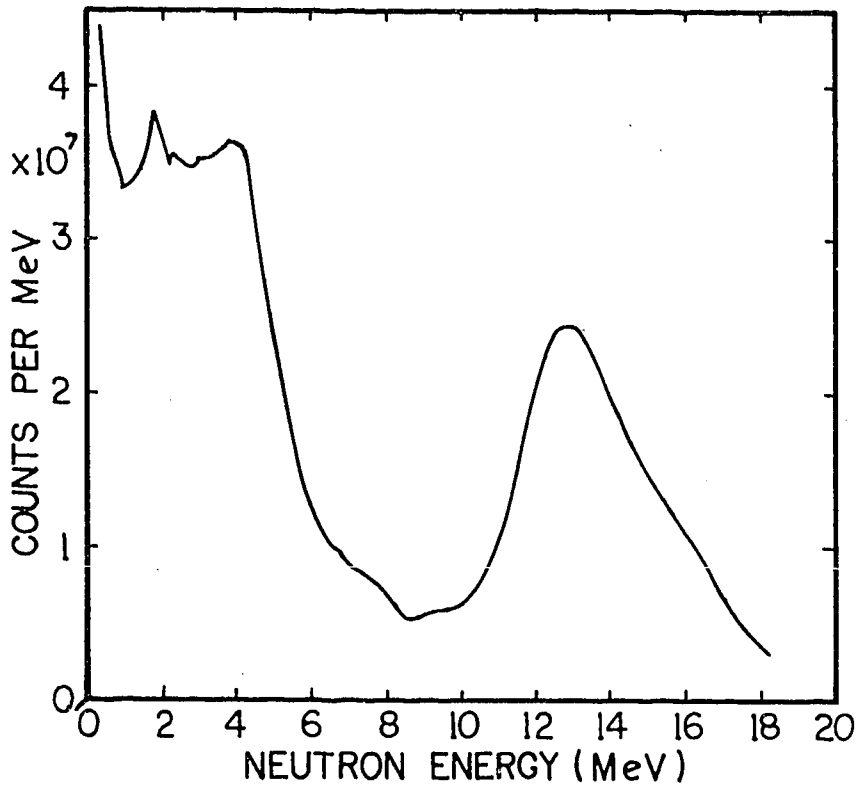

FIGURE 8. NEUTRON ENERGY SPECTRUM FROM A THICK NATURAL LITHIUM TARGET BOMBARDED BY 2.3 MeV DEUTERONS

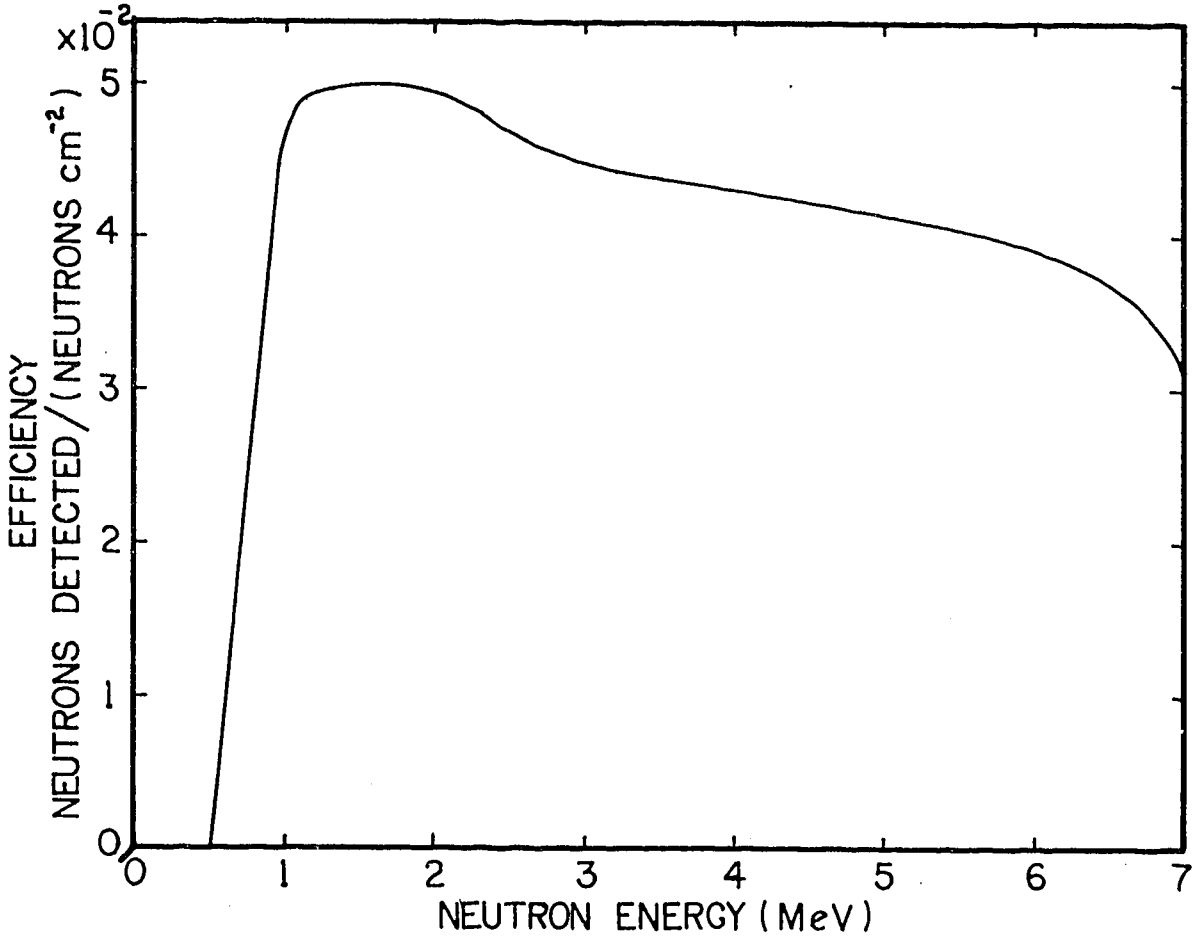

FIGURE 9. SCINTILLATOR PROBE EFFICIENCY

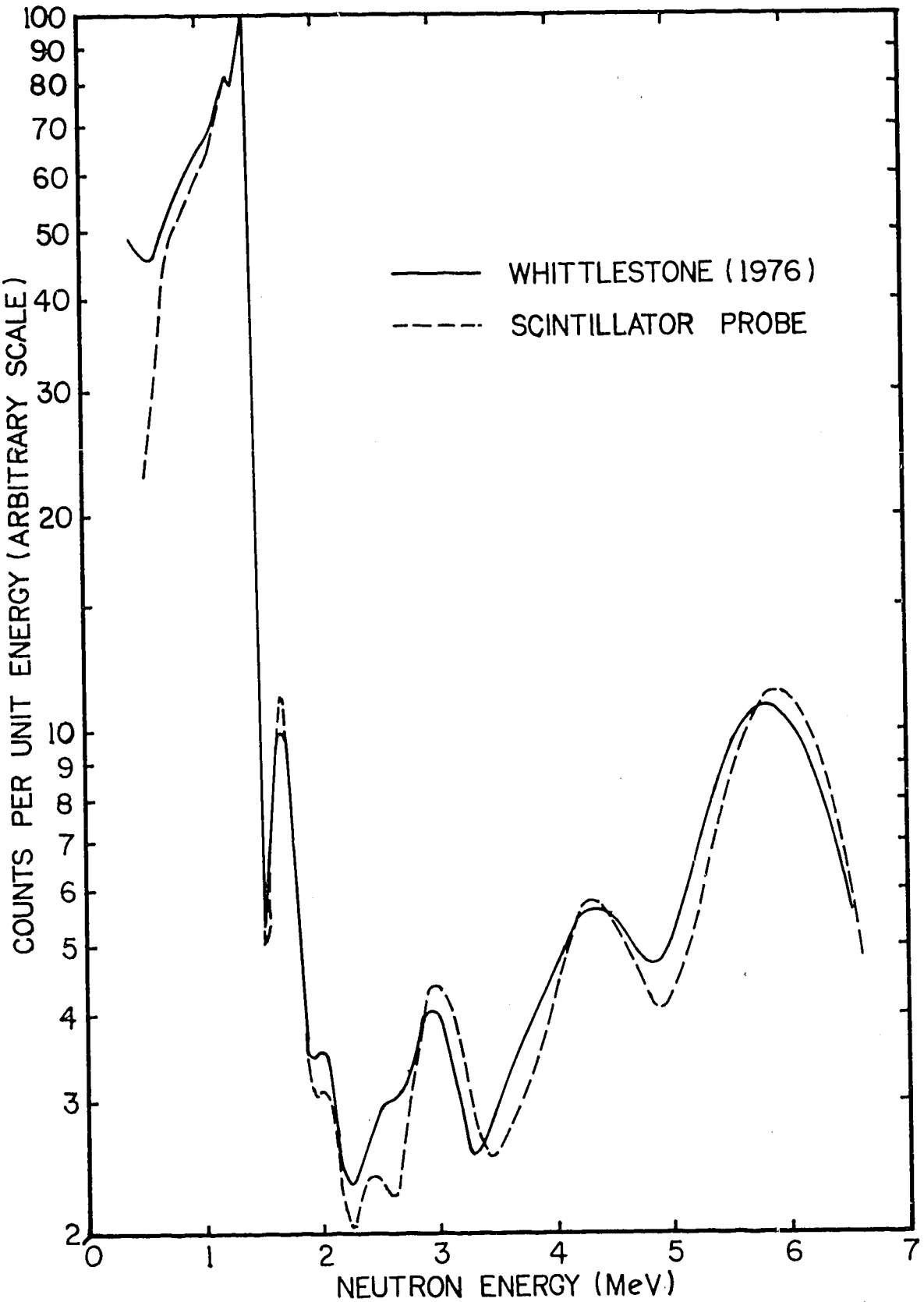

FIGURE 10. NEUTRON ENERGY SPECTRUM FROM A THICK BERYLLIUM TARGET BOMBARDED BY 2.3 MeV DEUTERONS

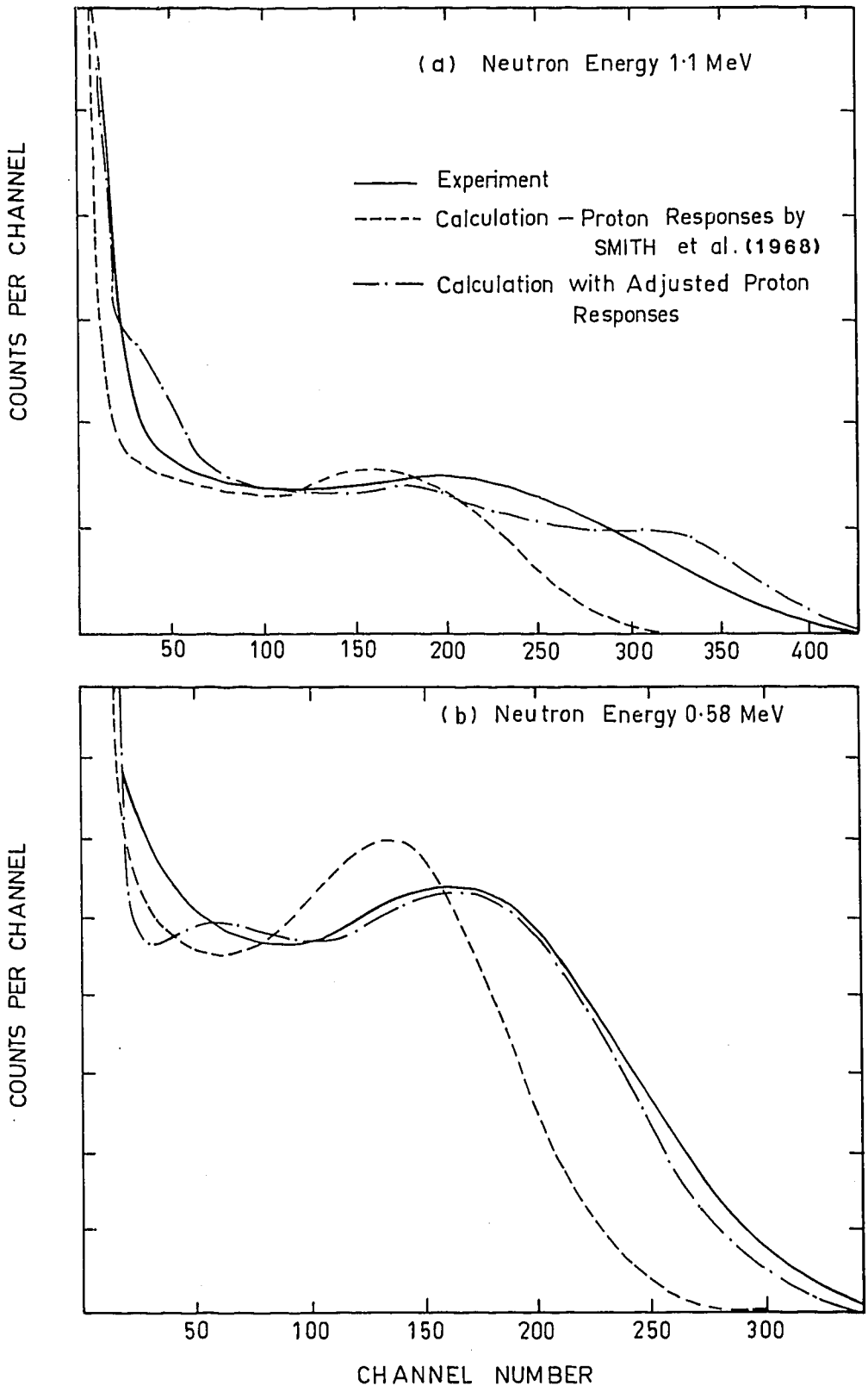

FIGURE 11. CALCULATED AND EXPERIMENTAL MONOENERGETIC NEUTRON RESPONSES - LARGE NE213 SCINTILLATOR

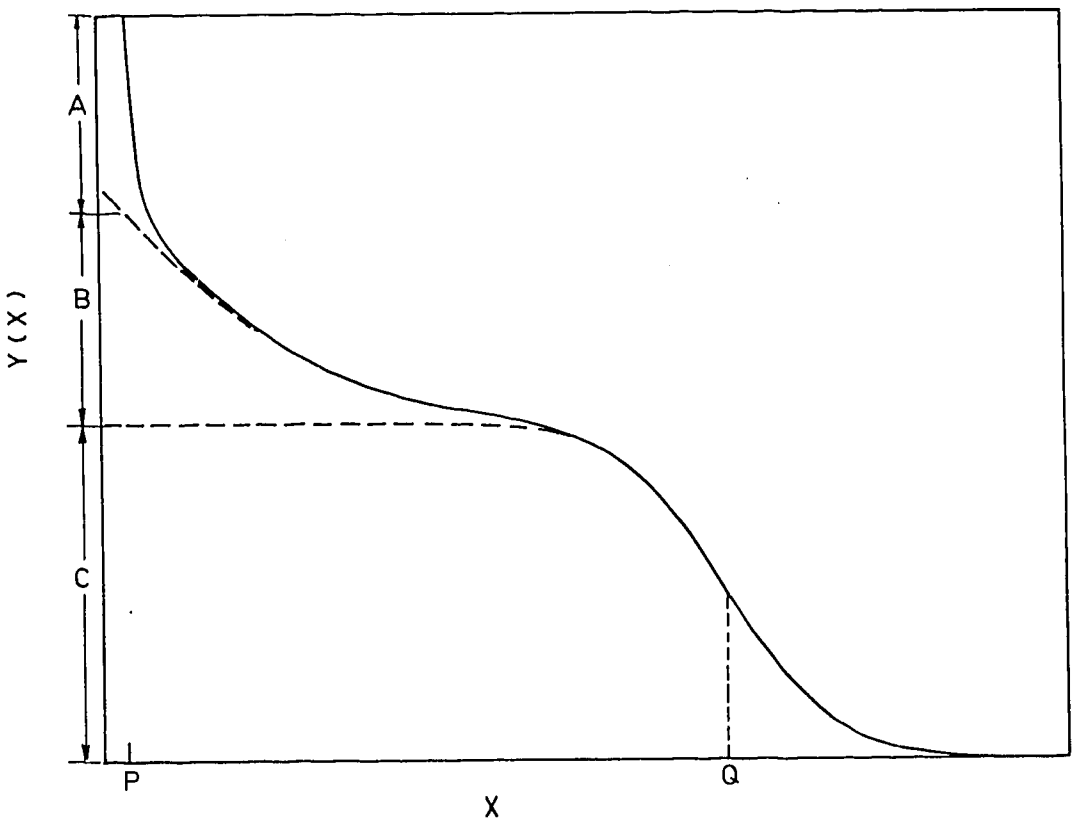

FIGURE 12a. THE FUNCTION $Y(X) = A.e^{T(P-X)} + B.e^{U(P-X)} + C.erf\left(\frac{Q-X}{S}\right)$

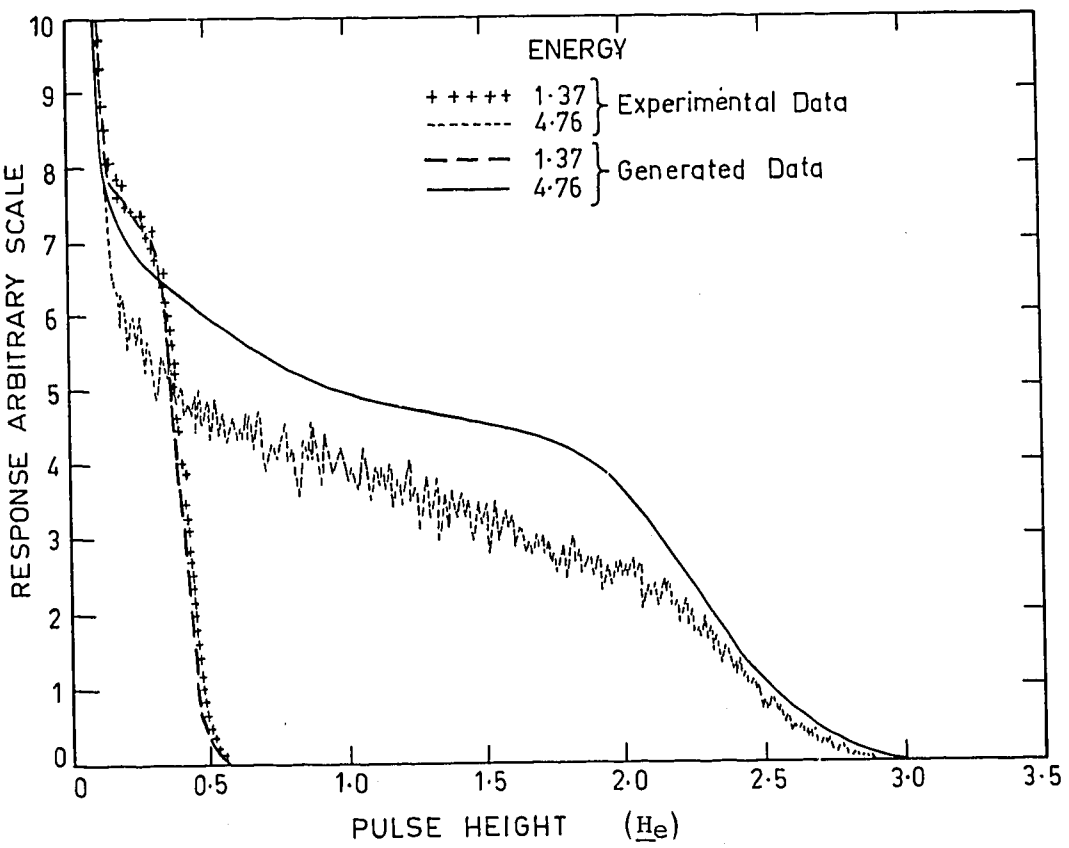

FIGURE 12b. EXPERIMENTAL AND GENERATED MONOENERGETIC NEUTRON RESPONSES - SCINTILLATOR PROBE

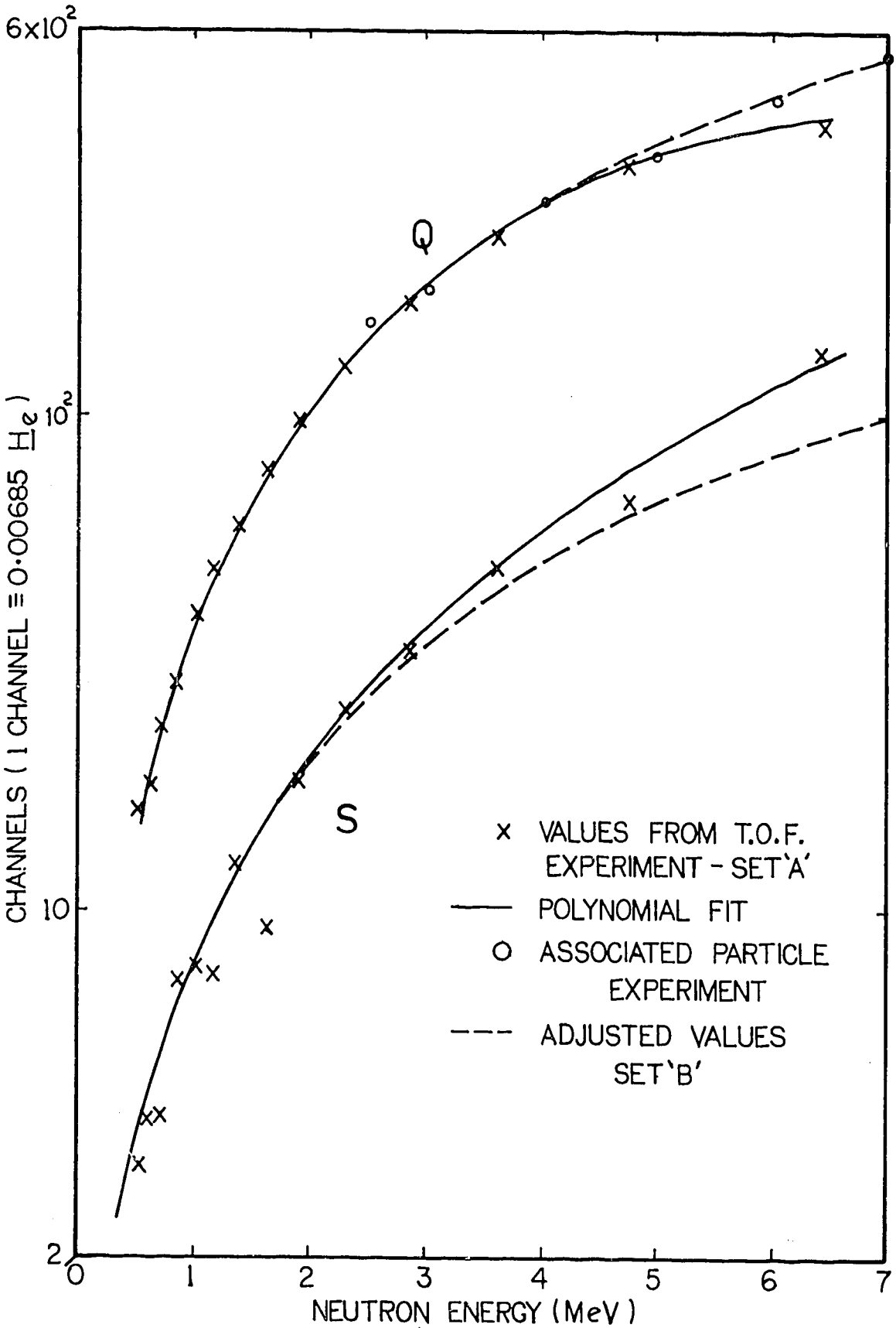

FIGURE 13. THE PARAMETERS 'Q' AND 'S' FOR RESPONSE SETS 'A' AND 'B' VERSUS NEUTRON ENERGY

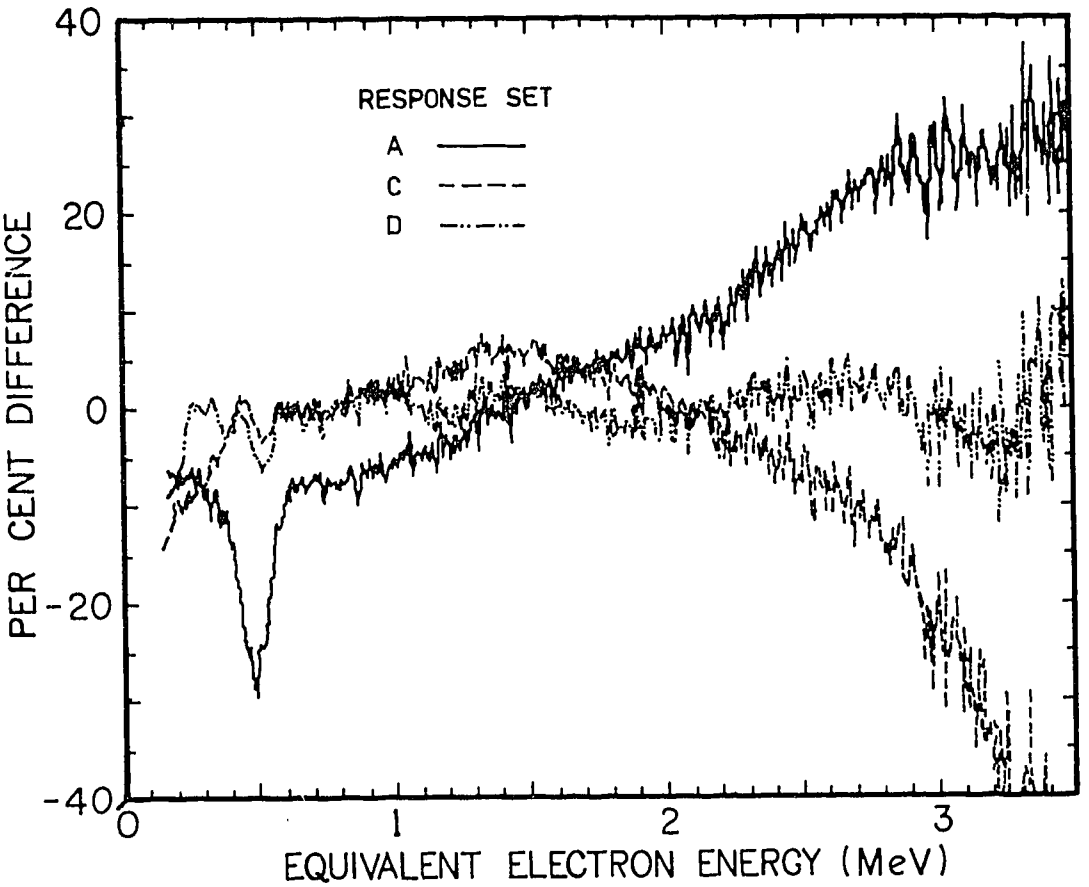

FIGURE 14. THE DIFFERENCE BETWEEN THE EXPERIMENTAL AND RECONSTRUCTED PULSE HEIGHT SPECTRUM USING A ^{9}Be (d,n) ^{10}B NEUTRON SOURCE

APPENDIX A
THE INDIUM-113m SOURCE

The ^{113m}In source was originally intended for use as a calibration source for the scintillation detectors. A drop of solution containing ^{113}Sn, which supports ^{113m}In, was allowed to dry on a platinum wire which was inserted into the scintillation chamber. By calculation, the energy loss by Auger electrons penetrating the evaporated material was less than 2 keV. Proof that the energy loss was low is supported by the width of the peak after subtracting the background. In the large chamber, the FWHM of the peak was just that amount due to the photomultiplier statistical broadening of a single intensity pulse from a light pulser. Despite this, the peak occurred at 0.34 $\underline{H}_e$ (Figure 3) instead of 0.392 $\underline{H}_e$, which would be expected if the whole energy of the internal transition were absorbed, or a little less if the K or L X-ray accompanying the electron escaped. An hypothesis to explain this discrepancy in energy is that the layer of scintillator adjacent to the surface of the platinum wire is effectively quenched and produces no light. Only after traversing a layer in which it loses about 50 keV does an electron enter a region of the scintillator where it can produce scintillations. This hypothesis remains to be proved.

APPENDIX B
EXPERIMENTAL DATA BASE FOR MONOENERGETIC NEUTRON RESPONSE DETERMINATION

B.1 TIME-OF-FLIGHT MEASUREMENT

The monoenergetic neutron response set A (Section 6) was measured at an elevated target facility described in detail elsewhere [Whittlestone 1977]. The accelerator beam was pulsed and the neutron energies were determined by measuring the flight time of the neutrons from the target to the detector. By analysing the pulse heights of neutron counts in a narrow range of times (a time window) after the beam pulse, a monoenergetic neutron response was obtained. The main parameters of the measurement were:

Target material:	lithium (thick)
Beam particles:	deuterons
Pulse width:	3 ns FWHM
Flight path:	1.90 m
Time windows:	width 3 ns

Energy range covered - 0.535 to 6.44 MeV

The neutron source was lithium bombarded by deuterons, chosen because the neutron output from the $^{7}Li(d,n)^{8}Be$ reaction is high and the energy spectrum smooth over the range of interest. Responses of monoenergetic neutrons with energies between 0.535 and 6.44 MeV could be obtained by accumulating pulse height spectra simultaneously from several time windows.

The resolution of the measurement was limited mainly by the 3 ns minimum pulse width from the accelerator and by the choice of flight path, which was a compromise between count rate and resolution. Although the measurements could have been made with double the flight path to improve the resolution, the resultant quadrupling of the count time and increase of scattered neutron background at the low energies were unacceptable.

A second compromise on resolution versus count rate was involved in the selection of the time window width at 3 ns, equal to the width of the beam pulse. It was considered that a reduction in resolution from about 4.2 to 3.4

ns was not worth the sacrifice of a factor of 2 in count rate obtained by reducing the window width to 1.5 ns.

Background from scattered neutrons, although small at the elevated target station, was evident in the low energy responses. It was possible to evaluate and correct for this background. From experiments using the elevated target station [Whittlestone 1977], it was known that the scattered component at any particular time had a fairly narrow energy distribution, centred on an energy substantially higher than that defined by the time window of interest for neutrons coming directly from the target. The pulse height distribution of the scattered component at each time was therefore known quite accurately from the higher energy responses obtained at earlier times. By matching the higher pulse height part of the response to the known higher energy response, it was possible to form an accurate estimate of the contribution to low energy responses from scattered higher energy neutrons (Figure B1). This contribution could then be subtracted.

B.2 ASSOCIATED PARTICLE MEASUREMENT

The associated particle technique was used to measure some monoenergetic neutron responses. The experimental rig was essentially that described by Jones et al. [1974] and was operated by one of the co-authors (C.M. Bartle), using a deuteron beam from the 6 MV tandem Van de Graaff accelerator at the Australian National University. Tritons and neutrons from a deuterated polyethylene target were detected, the former by a surface barrier detector and the latter by the scintillator probe. The energy of the neutrons was defined by the angle of emission and the incident deuteron energy. If the neutron detector had been larger than about 2.5 cm diameter, each triton detected would have been accompanied by a neutron passing into the neutron detector, permitting the absolute efficiency of the detector to be determined.

For measuring the responses of the scintillator probe, this associated particle rig was unsatisfactory in two respects. Firstly, the neutron beam was considerably larger than the scintillator, which meant that the absolute detection efficiency of the scintillator could not be determined. Secondly, the count rate was of the order of 1 s^{-1}, which made it quite impracticable to measure monoenergetic neutron responses to sufficient accuracy in the time available. However, a few responses were measured with very poor statistical accuracy. They showed that the resolution of the detector was in the range 4

to 8 per cent up to 12 MeV. It was evident that edge effects could be ignored for neutrons with energies of 6 MeV or less.

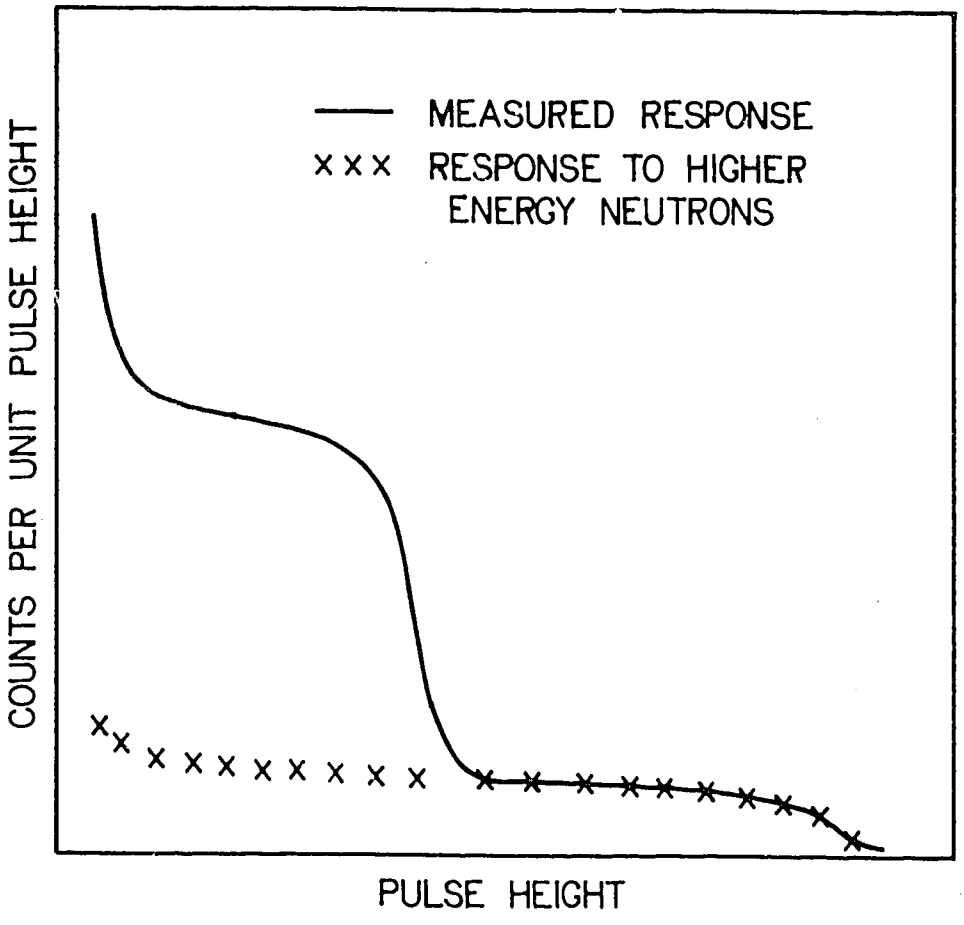

FIGURE B1. ILLUSTRATION OF BACKGROUND EVALUATION FOR MONOENERGETIC NEUTRON RESPONSES